SANDIA REPORT

SAND98–0547 • UC–910
Unlimited Release
Printed March 1998

CONF-970638--
CONF-9705237--

High-Speed Modulation of Vertical Cavity Surface Emitting Lasers

Vincent M. Hietala, Marcelino G. Armendariz, Kevin L. Lear, Kent D. Choquette

Prepared by
Sandia National Laboratories
Albuquerque, New Mexico 87185 and Livermore, California 94550

Sandia is a multiprogram laboratory operated by Sandia Corporation, a Lockheed Martin Company, for the United States Department of Energy under Contract DE-AC04-94AL85000.

Sandia National Laboratories

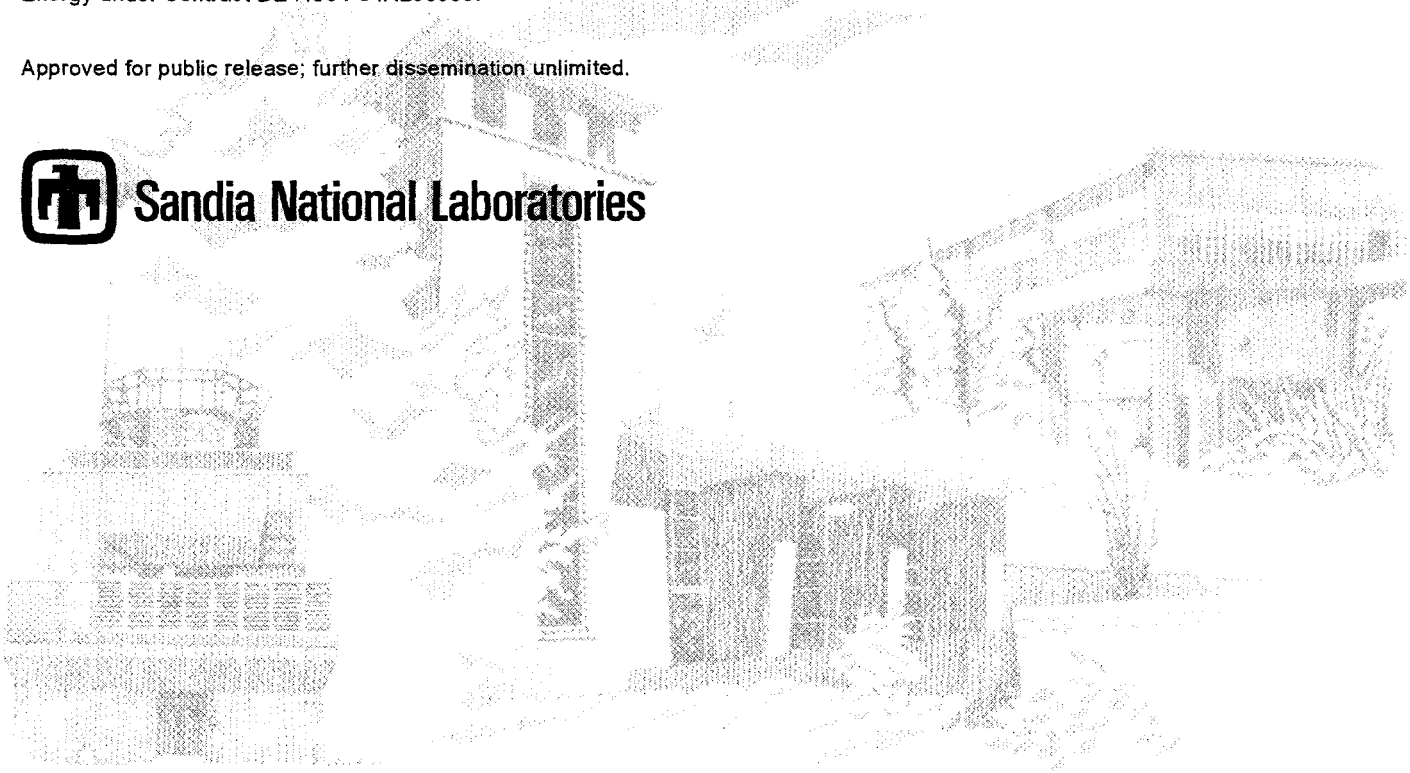

Issued by Sandia National Laboratories, operated for the United States Department of Energy by Sandia Corporation.

Available to DOE and DOE contractors from
Office of Scientific and Technical Information
P.O. Box 62
Oak Ridge, TN 37831

Prices available from (615) 576-8401, FTS 626-8401

Available to the public from
National Technical Information Service
U.S. Department of Commerce
5285 Port Royal Rd
Springfield, VA 22161

NTIS price codes
Printed copy: A03
Microfiche copy: A01

SAND98-0547
Unlimited Release
Printed March 1998

Distribution
Category UC-910

HIGH SPEED MODULATION OF VERTICAL CAVITY SURFACE EMITTING LASERS

Vincent M. Hietala, Marcelino G. Armendariz, Kent D. Choquette,
and Kevin L. Lear*

Microelectronics and Photonics Center

Sandia National Laboratories

P.O. Box 5800

Albuquerque, New Mexico 87185-0874

*Present Address: MicroOptical Devices Inc., 5601C Midway Park Pl. NE,
Albuquerque, NM 87109

Abstract

This report summarizes work on the development of high-speed vertical cavity surface emitting lasers (VCSELs) for multi-gigabit per second optical data communications applications (LDRD case number 3506.010). The program resulted in VCSELs that operate with an electrical bandwidth of 20 GHz along with a simultaneous conversion efficiency (DC to light) of about 20%. To achieve the large electrical bandwidth, conventional VCSELs were appropriately modified to reduce electrical parasitics and adapted for microwave probing for high-speed operation.

Acknowledgment

The authors are indebted to a multitude of researchers at Sandia and elsewhere, including: H. Q. Hou, B. E. Hammons, J. C. Zolper, A. Mar, S. P. Kilcoyne, M. Ochiai, F. Cajas, N. H. Berg, J. J. Banas, J. Figiel, G. Hammons, J. Nevers, and K. M. Geib.

This work was performed at Sandia, a multiprogram laboratory operated by the Lockheed Martin Company, for the United States Department of Energy under Contract DE-AC04-94AL85000.

Contents

Figures/Illustrations

Tables

I. Summary

This report summarizes work on the development of high-speed vertical cavity surface emitting lasers (VCSELs) for multi-gigabit per second optical data communications applications (LDRD case number 3506.010). The program resulted in VCSELs that operate with an electrical bandwidth of 20 GHz along with a simultaneous conversion efficiency (DC to light) of about 20%. To achieve the large electrical bandwidth, conventional VCSELs were appropriately modified (i.e. reducing electrical parasitics) for high-speed operation and adapted for microwave probing.

The principle portions of this report are two Appendices (A and B) which are reprints of two papers. Most of the important results from these two papers are summarized here. Additionally, Appendix C gives a short bibliography listing several recent publications which may be of interest for additional details.

To obtain record bandwidth and high efficiency performance, several novel process and material variations were required. These included careful design of the epitaxial mirrors for minimization of resistance; n-type mirror up design to lower effective contact resistance; selective wet oxidation for improved mode confinement; and thick polyimide planarization under the contact pads along with an additional proton implantation to lower parasitic device capacitance. Details of these and other improvements can be found in Appendix A and B. These device improvements moved the electrical RC bandwidth above 30 GHz. With this large RC bandwidth, electrical parasitics no longer were the mechanism limiting the VCSEL's bandwidth. The selective wet oxidation had the additional benefit of significantly increasing the device's intrinsic electrical bandwidth as well as increasing the VCSEL's efficiency. In fact , estimates of the intrinsic bandwidths of the VCSEL ranged from 58 GHz (Appendix B) to 90 GHz (Appendix A) based on small-signal bias-dependent measurements. These large intrinsic bandwidths were not attainable in practice due to thermal effects which were confirmed by VSCEL characterization over temperature from -50° C to +100° C (see Appendix B). Thus, improved thermal management is believed key to future speed increases.

Small-signal on-wafer measurements of the VCSEL were performed up to 30 GHz. These included both impedance and response measurements. A detailed small-signal RF model of the VCSEL was developed. This model accurately describes the electrical and optical characteristics of the VCSEL. Large signal operation of the VCSEL was demonstrated and characterized by using two-tone (3rd order intercept) and bit-error rate testing to 12.5 Gbps (gigabits per second). The devices appear suitable for operation in communication links at speeds in excess of 10 Gbps. Results of this modeling effort provides adequate design information for the application of VCSELs in communication systems. Details of this work can be found in Appendix A.

The important issue of appropriate pre-bias (off-state current) was explored and results are given in both Appendices A and B. In general, it was found that VCSELs require pre-bias considerations similar to traditional edge emitters. Interesting correlations between device size and on-off delays can be found in Appendix B.

Another aspect of this program's attempt to make a VCSEL useable for communication applications, was to demonstrate a robust packaging approach. A VCSEL package was developed and an 8 GHz bandwidth VCSEL was packaged for testing. A photograph of the packaged VCSEL is shown in Illustration 1. The package utilized standard microwave design techniques for the electrical signal and the optical connector was positioned for maximum optical coupling. The measured high-speed response is shown in Illustration 2. Good electrical bandwidth was maintained after packaging with reasonable optical output power.

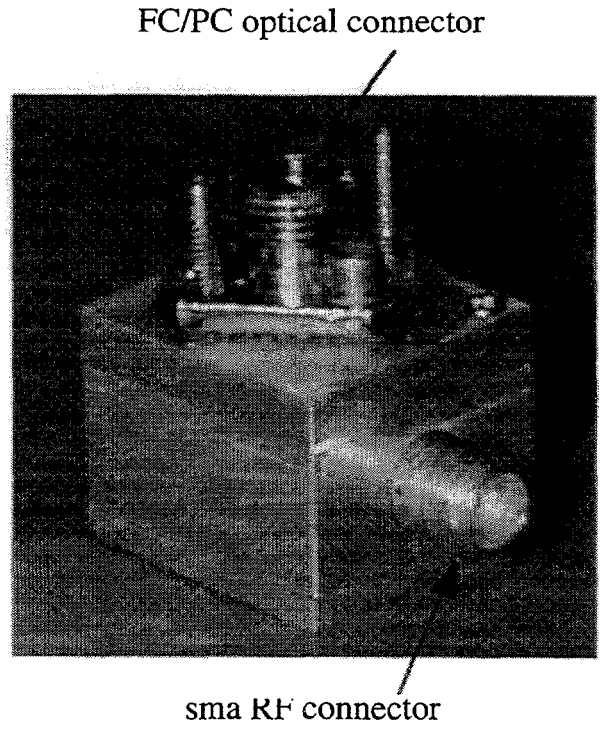

Illustration 1. Photograph of the completed packaged VCSEL assembly.

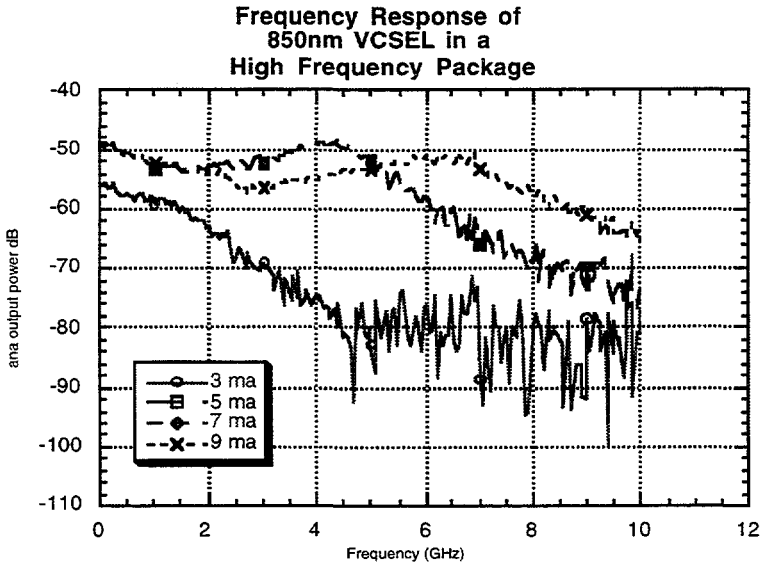

Illustration 2. Measured frequency response of the packaged 850 nm VCSEL.

II. Conclusions

High-speed VCSELs with very large electrical bandwidths and high conversion efficiencies have been successfully demonstrated. Both small and large signal effects have been investigated and current designs appear to be useable to bit rates in excess of 10 Gbps. The intrinsic speed limit of the device is believed to be significantly higher than present measured extrinsic performance and is believed presently limited by thermal effects. Future designs with improved thermal management, lower device parasitics, and improved mode confinement are expected to produce VCSELs with modulation bandwidths in excess of 40 GHz.

CONF-970638--

Appendix A. Reprint of "Electrical Characterization and Application of Very High Speed Vertical Cavity Surface Emitting Lasers (VCSELs)"

1997 IEEE MTT-S International Microwave Symposium Digest, Denver, CO, pp. 355-358, June 10, 1997.

Electrical Characterization and Application of Very High Speed Vertical Cavity Surface Emitting Lasers (VCSELs)

V. M. Hietala, K. L. Lear, M. G. Armendariz, C. P. Tigges, H. Q. Hou, and J. C. Zolper

Sandia National Laboratories

Albuquerque, NM 87185-0874

Abstract

Vertical Cavity Surface Emitting Lasers (VCSELs) offer many benefits over conventional edge-emitting lasers including economical microelectronic batch processing, easy extension to 2-D arrays, and of interest here, very large intrinsic bandwidths due to reduced cavity volume. Results of electrical characterization of a 19 GHz bandwidth 850 nm VCSEL are presented. Small-signal characterization and modeling of the frequency response and device impedance is presented. Large signal performance is studied using two-tone RF and high-speed digital measurements. Appropriate drive conditions for high-speed digital applications are demonstrated.

Introduction

Very high efficiency VCSELs with over 20 GHz electrical bandwidths have been demonstrated with several mW output power. These are believed to be the fastest laser diodes ever realized at 850 nm. Though this wavelength is not consistent with long-haul optical link needs, it is consistent with the Fibre Channel and ATM Forum standards and is in strong favor for economical short haul fiber optic links.

The small cavity volume of VCSELs allows for very large intrinsic bandwidths. By the careful minimization of electrical parasitics, we have successfully demonstrated VCSELs with bandwidths in excess of 20 GHz. [1] This has been achieved by using several novel process enhancements. Intrinsic device limits appear to be well in excess of 50 GHz. It appears that the present bandwidth is limited predominantly by thermal issues.

Device Structure

A schematic diagram of the cross section of the high speed VCSEL is shown in Fig. 1. The VCSEL cavity is formed by MOVPE growth where an active region is appropriately positioned between two dielectric mirror stacks. The active region is comprised of five

GaAs quantum wells. The mirrors are necessarily comprised of alternating layers of high and low Al fraction AlGaAs for high optical reflectivity. This need typically results in an undesirably high mirror resistance (due to heterojunction barriers) which significantly degrades device performance. To minimize this effect, a novel uniparabolic grading profile produced by MOVPE growth as well as careful doping considerations were used to greatly reduce the mirror resistance [2] To further minimize mirror resistance, the VCSEL was grown n-type up (see Fig. 1) to take advantage of the lower lateral resistance of the n-type material.

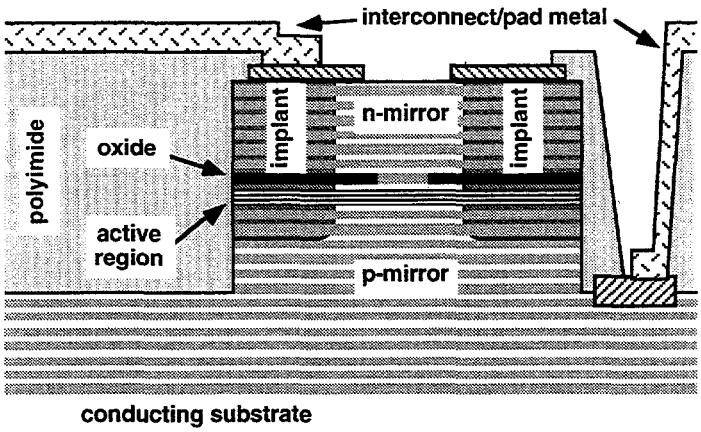

Fig. 1. Diagram of the VCSEL's cross section.

Another unique feature of these VCSELs is the use of a selective wet thermal oxidation used to convert an AlGaAs mirror layer to an insulating low index alumina film.[3] The low index of the resulting alumina layer yields excellent lateral mode confinement and overlap with the electrical pump; and lasers with 50% power efficiency have been demonstrated.[4]

Shown in Fig. 2 is a microphotograph of an actual 4x4 μm^2 device. Contact to the device is achieved by coplanar contacts. These contact pads are fabricated on top of a 4 μm thick polyimide layer which results in a low pad capacitance of about 50 fF. To further reduce the total device capacitance, a proton implant was performed under the contact regions (see Fig.1).

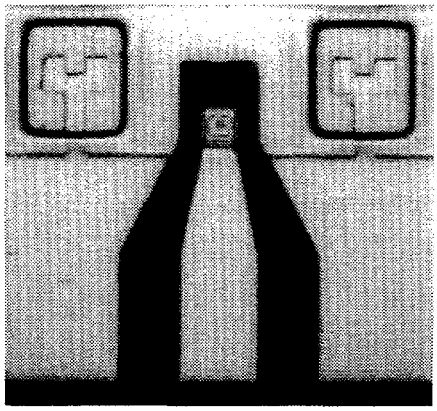

Fig. 2. Microphotograph of high-speed VCSEL. The VCSEL's 4x4 μm^2 aperture is the small dot seen at the end of the center strip.

All of the measurements in this paper were performed on-wafer using a standard RF probe and a lensed multimode fiber positioned normal to the DUT by using a Cascade Microtech lightwave probe. The light was detected using a 25 GHz bandwidth model 1431 New Focus detector.

Fig. 3 shows plots of the light in the fiber (estimated based on the detector's responsivity specification) and voltage for a 0 to 6 mA current bias range. Note the very low threshold current (≈0.5 mA) and the low operating voltage.

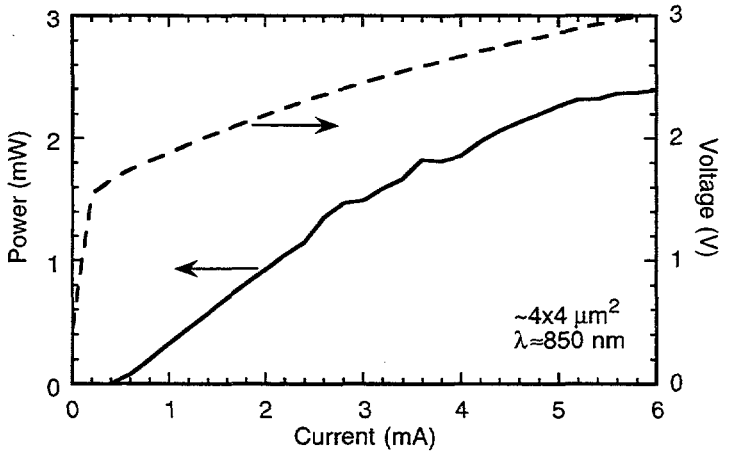

Fig. 3. Light (in fiber) and voltage over bias current.

Small-Signal Model

Small-signal characterization was performed with an HP 8510 network analyzer using an LRM calibration for the impedance measurements and a simple response calibration along with correction for probe loss and detector response for the response measurements.

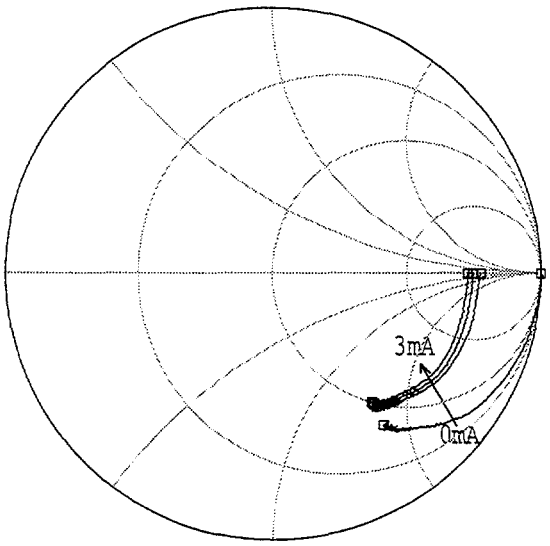

Fig. 4. Measured S11 of the VCSEL at 0, 1, 2, and 3 mA bias currents (0.045 to 25 GHz).

Plotted in Fig. 4 is the measured S11 for several different bias currents. Due to the small size of these VCSELs and the mirror resistance, electrical drive impedances are much higher than with conventional edge emitter lasers.

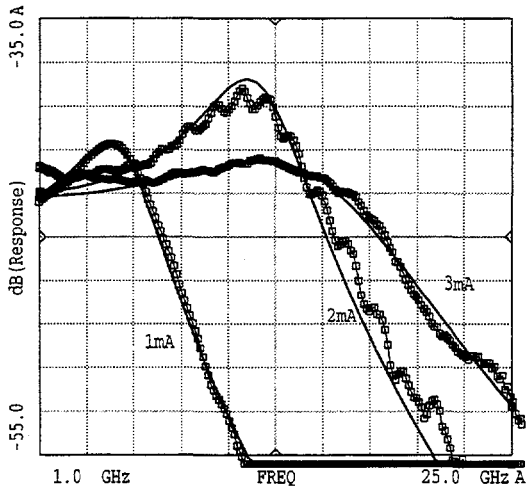

Fig. 5. Modulation response of a high speed VCSEL exhibiting a 19 GHz - 3 dB frequency. Curves are for 1, 2 and 3 mA bias as labeled.

Fig. 5 shows the measured response along with corresponding fits using the small-signal model outlined in Fig. 6. A co-optimization was used to simultaneously fit the measured S11 and response. In general, the modeled S11 results (not shown in Fig. 4 for clarity) were very similar to the measured. From a co-optimization at several bias conditions C_p=54 fF, R_p=16 Ω, and R_m=136 Ω. The active region's equivalent capacitance, C_a and equivalent resistance, R_a were found to be bias dependent with R_a varying from 270Ω at 1mA to 160Ω at 5 mA and C_a varying from 67 fF at 1 mA to 106 fF at 5 mA. These values for R_a may seem large as compared to a normal junction resistance, but this resistance includes a combination of lateral and spreading terms.

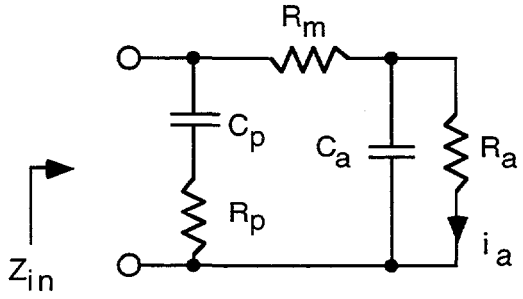

$$\frac{I_o}{i_a} = \frac{G}{(s-s_o)(s-s_o^*)}\bigg|_{s_o=\Gamma+j\omega_o} = \frac{G(\Gamma^2+\omega_o^2)}{s^2+2\Gamma s+\Gamma^2+\omega_o^2}$$

C_p = *Pad Capacitance*	R_p = *Pad Loss*
R_m = *Mirror Resistance*	C_a = *"Active" Capacitance*
R_a = *"Active" Resistance*	G = *Scaling Constant*
Γ = *Resonance Width*	f_o = *Relaxation Frequency*

Fig. 6. Small-signal VCSEL equivalent circuit. The differential light output, I_o, is modeled using the traditional damped resonator model.

Fig. 7 shows a plot of the measured cutoff frequency, f_{-3dB}; the relaxation frequency, f_o; and the resonance width $\Gamma/2\pi$ (defined in Fig. 6) plotted against bias current. At low bias currents, from conventional rate equation analysis, the 3dB bandwidth is known to increase in proportion to the square root of the drive current above threshold. For the data in Fig. 7, the resulting modulation current efficiency factor is about 15.2 GHz/√mA. The resonant frequency, f_o, is seen to increase rapidly at low bias currents and then quickly saturate at about 3 mA to around 16 GHz. This is a clear indication of a limit due to heating in the device. A quadratic fit of the damping rate, Γ, against the resonant frequency, f_o, at resonant frequencies below 15 GHz, results in K factor of 95 pS which implies an intrinsic bandwidth in excess of 90 GHz. Such frequencies are not currently attainable due to thermal effects, and remaining device RC parasitics. If these issues could be minimized along with designs for single-mode operation at extended bias currents, it is believed that significant bandwidth increases could be realized.

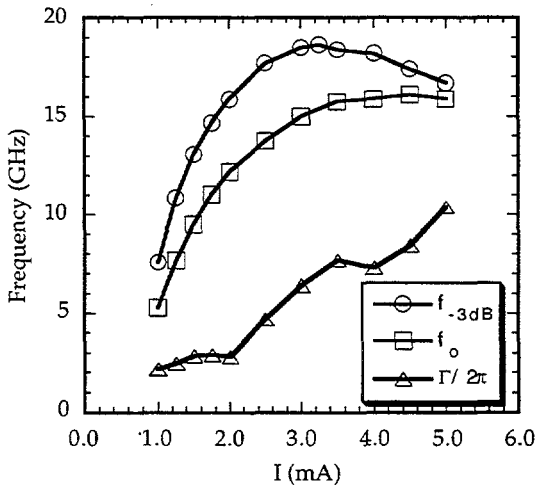

Fig. 7. The cutoff frequency, f_{-3dB}; the extracted relaxation frequency, f_o; and the extracted resonance width $\Gamma/2\pi$ plotted versus bias current.

Large Signal Operation

To evaluate large signal operation, two-tone tests and digital measurements were performed. Fig. 8 shows the result of a two-tone test performed at 5 GHz with a device bias current of 3.75 mA. The linear components (at 5 and 5.01 GHz) and the 3rd order inter-modulation components were seen to both increase at the proper rate (1dB/dB and 3dB/dB). The vertical scale in this plot represents the actual power levels measured on a spectrum analyzer. The scale is relative as the fiber coupling can be arbitrarily adjusted and hence absolute power measurements are difficult. Nevertheless, the intercept from the horizontal axis (6.5dBm) gives a good indication of suitable drive levels for low distortion analog link applications. The spurious free dynamic range for this fiber optic link is over 40 dB at optimal bias. This intercept is bias dependent with a measured values of 7 dBm, ≈16 dBm, and 6.8 dBm at bias currents of 1.25, 2.5 and 3.75 mA, respectively at 5 GHz. Measurements at the mid bias range, were difficult due to the small 3rd order component even when driving the device at power levels approaching the 1dB compression point (around -3 dBm). As expected distortion occurs at either bias extreme.

Fig. 9 shows scope traces of the output light with the VCSEL driven with a 10 GHz square wave and at different bias levels. The top trace shows operation at a point too close to the threshold current, resulting in severe distortion. The middle trace shows operation at

an idle current which is more suitable, though ringing still occurs due to the limited optical damping at low drive currents. Finally, the lower trace shows operation a 3 mA bias current which results in a faithful reproduction of the drive signal.

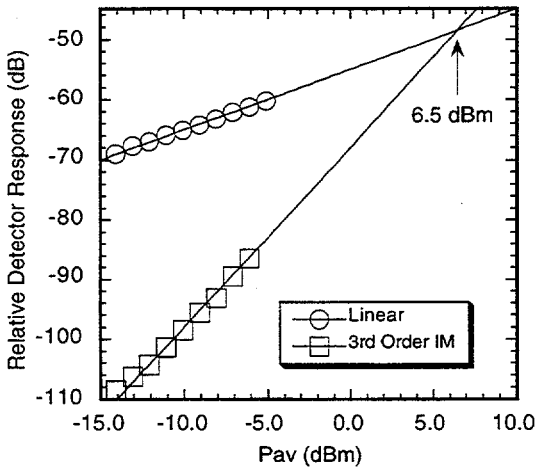

Fig. 8. Measured linear (5.01 GHz) and 3rd order (5.02 GHz) product versus unmatched average input power.

Fig. 10 shows an eye diagram at 10 Gbps (2^8-1 sequence) with a reasonable eye width. Part of the noise seen in Fig. 10 is electrical noise caused the measurement system (detector is operated directly into the oscilloscope).

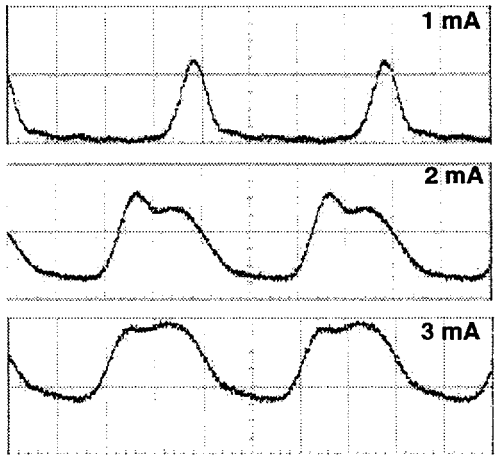

Fig. 9. VCSEL light emission with a 10 Gbps ECL-level square wave excitation at 1, 2, and 3 mA bias currents. Bottom of scale is no light. Top is VCSEL light level at 4.4 mA drive.

Conclusions

Electrical characterization of a very large bandwidth VCSEL laser was presented. Both small and large signal effects have been investigated. Current designs appear to be useable to bit rate speeds in excess of 10 Gbps. The intrinsic speed limit of the device is believed to be significantly higher than present measured extrinsic performance. Future designs with improved thermal management, lower device parasitics, and improved mode

confinement are expected to produce bandwidths well within the millimeter wave frequency regime.

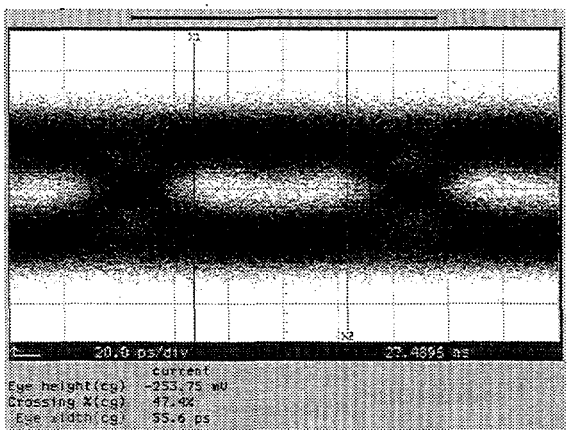

Fig. 10. Eye diagram of a VCSEL driven at 10 Gbps by a 50Ω impedance ECL-level source. DC bias level was 3 mA.

Acknowledgments

The authors thank F. Cajas, J. Banas, J. Figiel, G. Hammons, S. Kilcoyne, and J. Nevers for their technical assistance.

This work was supported by the U. S. Department of Energy under contract #DE-AC04-94AL85000. Sandia is a multiprogram laboratory operated by the Sandia Corporation, a Lockheed Martin Company, for the United States Department of Energy.

References

[1] K. L. Lear, H. Q. Hou, V. M. Hietala, K. D. Choquette, and R. P. Schneider, Jr., "Engineering high-performance vertical cavity lasers," will be published in the Proceedings of the IEEE, COMMAND '96, Canberra, Australia, Dec. 8-11 1996.

[2] K. L. Lear, and R. P. Schneider, Jr., "Uniparabolic Mirror Grown by Molecular Beam Epitaxy," Appl. Phys. Lett., vol. 62, pp. 1585-1587, 1993.

[3] K. D. Choquette, R. P. Schneider, Jr., K. L. Lear, and K. M. Geib, "Low Threshold Voltage Vertical-Cavity Lasers Fabricated by Selective Oxidation," Electron. Lett., vol. 30, 00. 2043-2044, 1994.

[4] K. L. Lear, K. D. Choquette, R. P. Schneider Jr. , S. P. Kilcoyne, and K. M. Geib, "Selectively oxidized vertical cavity surface emitting lasers with 50% power conversion efficiency," Electron. Lett., vol. 31, pp. 208-209, 1995.

CONF-9705237--

Appendix B. Reprint of "Small and Large Signal Modulation of 850 nm Oxide-Confined Vertical Cavity Surface Emitting Lasers"

Presented at CLEO, Baltimore, MD, May 18, 1997.

Small and Large Signal Modulation of 850 nm Oxide-Confined Vertical Cavity Surface Emitting Lasers

K. L. Lear, V. M. Hietala, H. Q. Hou, M. Ochiai,

J. J. Banas, B. E. Hammons, J. C. Zolper, and S. P. Kilcoyne

Sandia National Laboratories, PO Box 5800 / MS 0603, Albuquerque, NM 87185-0603

Abstract

The high speed performance of GaAs quantum well, oxide-confined, vertical cavity surface emitting laser diodes is presented. Ion implantation reduces device capacitance resulting in small signal modulation bandwidths up to 21.5 GHz. Analysis and temperature dependent data show the lasers are thermally rather than intrinsically limited. Large signal data rates up to 12 Gb/s are presented including pattern dependent jitter resulting form variable turn-on delay.

Key Words

VCSEL; High speed laser diodes; Microwave frequency response

Introduction

VCSELs are attractive sources for high data rate, economical, fiber communications in local area networks and other applications with rapidly growing bandwidth requirements. We have previously demonstrated record modulation bandwidths for oxide-confined vertical cavity surface emitting lasers (VCSELs) based on strained InGaAs/GaAs quantum wells[1]. The monolithic oxide-confined structure[2] provides good optical confinement, low thresholds, efficient operation, and acceptable thermal resistance; these qualities promote high speed operation. Here we report work on nominally 850 nm wavelength oxide-confined VCSELs with modulation bandwidths in excess of 20 GHz. This shorter wavelength is more attractive because of its greater compatibility with data communications standards. Large signal modulation appropriate to such systems is also discussed below. In particular, the limitations imposed by turn on delay for various bias conditions are quantified for this type of VCSEL structure.

Laser Structure

High modulation bandwidths were achieved with an oxide confined VCSEL structure modified to decrease parasitic circuit elements. The devices reported here utilized an inverted doping approach detailed previously[3] with the n-mirror above the active region to reduce resistance and promote single mode operation by reducing current crowding. Figure 1 shows a schematic cross section of the VCSEL with a corresponding small signal equivalent circuit. Coplanar waveguide pads designed for on wafer probing were placed on a 5 μm thick polyimide to reduce the capacitance between the pad and the conducting

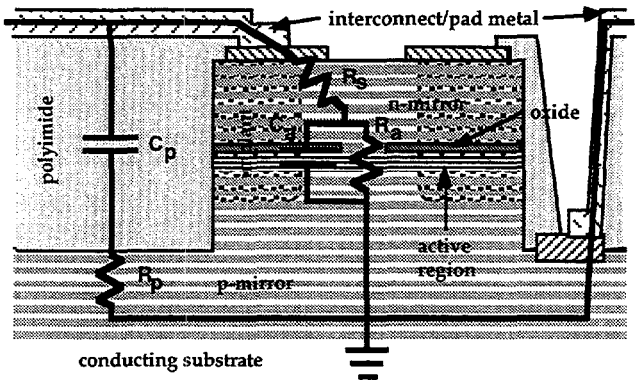

Figure 1. Schematic cross section of high speed VCSEL structure with superposed equivalent circuit.

substrate to approximately 50 fF. The device capacitance was further reduced by implanting the mesa area lying outside the active region where thin oxide layers would otherwise result in high capacitance. The electrical effects of the implant were evaluated by looking at the changes in the laser's microwave vector impedance. The magnitude and phase of the associated reflection coefficient are plotted in Figure 2. Device capacitance is evident in the phase change with frequency. Higher levels of implantation decrease the phase change associated with the capacitance.

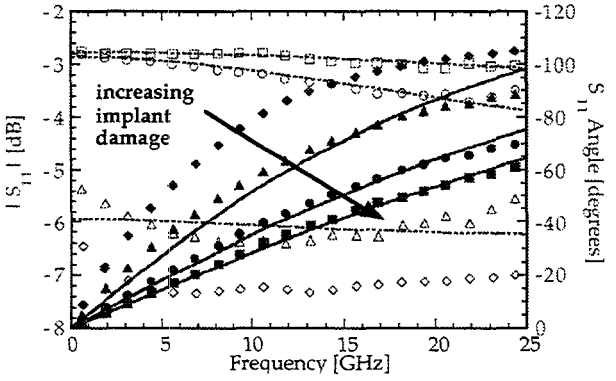

Figure 2. The magnitude (open symbols) and phase (closed symbols) of a small VCSEL's impedance at microwave frequencies. Lines show equivalent circuit fits.

This is quantified by adjusting the parameters of the equivalent circuit in Figure 1 to obtain a fit to the data of Figure 2. The resulting parameters are presented in Table 1 showing that the capacitance is clearly reduced by implantation. The implants also increase the resistances, but the net effect is an increase in electrical bandwidth. At low levels of implant, the maximum observed laser bandwidth is comparable to the electrical bandwidth. At higher levels the observed bandwidth becomes larger than the calculated bandwidth indicating the laser is no longer principally limited by electrical circuit effects.

Table 1. Equivalent circuit parameters for different levels of implants and corresponding calculated electrical bandwidth.

Implant Level	R_s [Ω]	R_a [Ω]	C_a [fF]	$f_{-3dB,elec}$ [GHz]
low	31.3	120.4	152.1	18.8
medium	36.3	269.6	72.9	25.8
high	28.3	288.7	44.3	36.4

Data taken at 2V bias. The pad capacitance and associated resistance were taken as C_{pad}=41.65 fF and R_{pad}=15.9 Ω based on measurements of an isolated pad.

The implant may also enhance the high speed performance by providing recombination centers that reduce the charge storage in the area just outside the oxide aperture. The reduced carrier levels also increase perimeter optical loss encouraging extended single mode operation.

The laser diodes feature DC characteristics that are important for high speed modulation as well. Figure 3 shows quasi-static light-current and voltage-current characteristics indicating a submilliampere threshold current, operation to several times threshold before thermal rollover, good efficiency coupled into the fiber, and moderate resistance for this size of device (~4x4 μm^2). This device operated in the fundamental mode to approximately 4 mA as necessary to obtain increasing photon densities in the mode. Other similar sized devices remained single-mode at all operating currents.

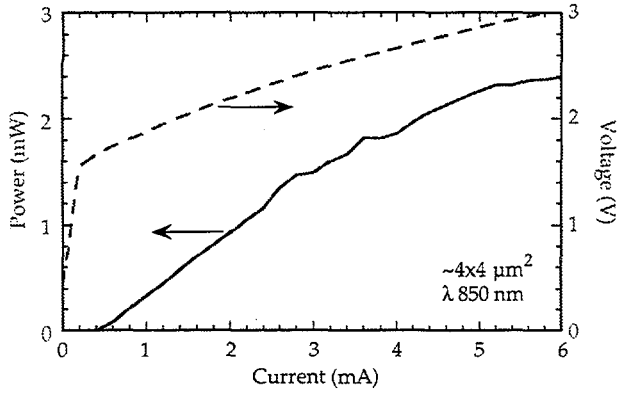

Figure 3. Fiber coupled power and voltage vs. current for a high speed single mode VCSEL.

Small Signal Modulation

The small signal response of VCSELs as a function of bias current was measured using a calibrated vector network analyzer with on wafer probing and a 30 GHz photodetector connected through approximately 2 m of the multimode fiber. The modulation response of a ~4x4 μm^2 single mode laser with a 0.5 mA threshold current is shown in Figure 4 for various bias currents. This optical link reached a maximum bandwidth (3 dB down from the low frequency response) of 21.5 GHz at a bias current approximately ten times threshold. Typical maximum bandwidths were 19 GHz or higher. The droop in response at low (< 5 GHz) frequencies may be partially attributed to the detector performance. A 1.5 dB decrease was measured for the detector at a 1300 nm wavelength using a lightwave analyzer. This detector response has not been factored out of the data.

The data of Figure 4 was fit with a traditional damped resonator model to extract the resonant frequency and equivalent damping frequency ($\gamma/2\pi$) as shown in Figure 5. A $f^{0.1}$ factor was included to account for the low frequency droop and thus improve the fit. At low bias currents, the bandwidth and resonant frequency increase in proportion to the square root of the current above threshold as expected from the conventional rate equation analysis. The rate of increase in this region yields a modulation current efficiency factor (MCEF) of 14.2 GHz/√mA which is slightly lower than the highest value we previously reported for oxide confined VCSELs with InGaAs quantum wells[1]. Other workers have also obtained an 14 GHz/√mA

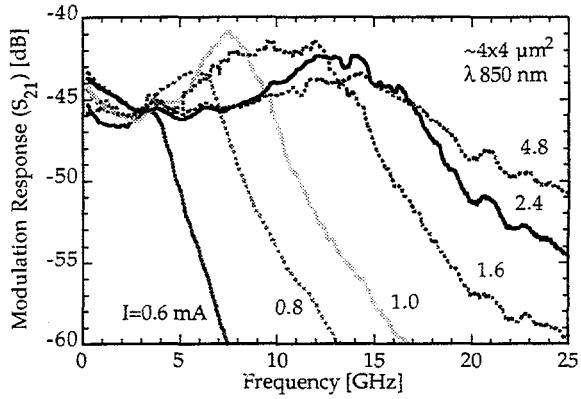

Figure 4. The modulation response of a single mode VCSEL for varying bias currents.

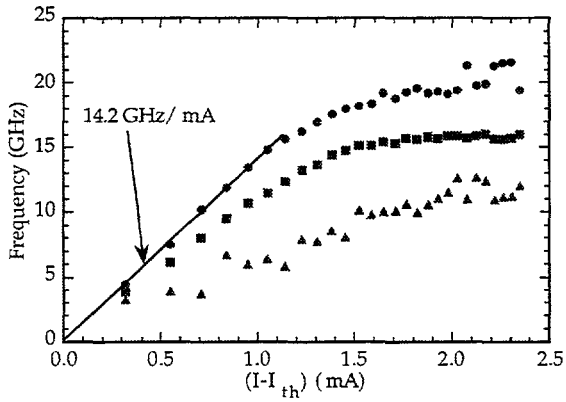

Figure 5. Resonance frequency (squares), -3dB frequency (circles), and equivalent damping frequency ($\gamma/2\pi$) (triangles) as a function of square root of current above threshold.

MCEF and a maximum 15.1 GHz bandwidth from an InGaAs VCSEL biased at 2.1 mA[4]. Here the bandwidth increases steadily to 15.5 GHz at 1.7 mA and then begins to saturate. Based on the damping factor's parabolic dependence on the resonant frequency, the intrinsic limits of the laser diode can be extrapolated from the data prior to saturation. This analysis yields a factor of K=0.159 ns which in conjunction with an zero current intercept of the

damping constant γ_0=18.8/ns predicts an intrinsic bandwidth limit of 58 GHz. The deviation from linearity in the light vs. current curve in Figure 3 above 4 mA can be attributed to thermal effects and further suggests that the saturation in bandwidth in a similar regime may be associated with decreased differential gain due to self-heating.

This conclusion is further supported by temperature dependent measurements. A nominally identical laser to that discussed above was characterized in wafer form on a variable temperature chuck. The bandwidth as a function of current extracted from this data is plotted in Figure 6 for varying temperatures. At 25 C, the bandwidth is similar to that for the preceding room temperature measurements. A higher ambient temperature shifts the internal temperature upward so that bandwidth saturation occurs with less self-heating and thus at lower currents where the bandwidth is reduced. Nevertheless, the laser still operates to 15 GHz at 100 C and corresponds to the bandwidth performance of the laser at 25C at lower currents. At both 25 and 100 C, the laser reaches 10 GHz with a bias current of approximately 1.1 mA. Lower stage temperatures extended the current range prior to self-heating

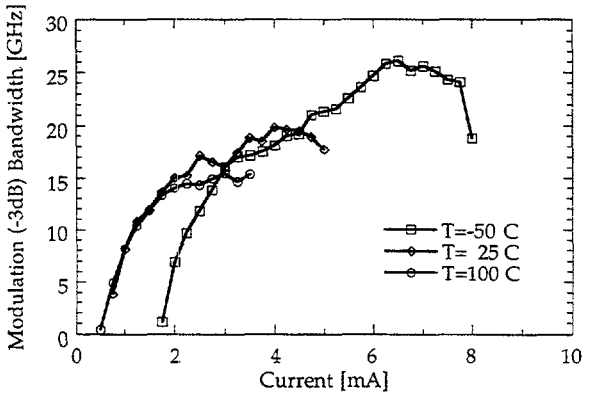

Figure 6. VCSEL bandwidth vs. current bias at three temperatures.

induced bandwidth saturation so that at -50C the laser attains a bandwidth of 26 GHz. At this temperature increased threshold current is necessary to heat the device sufficiently to shift the gain and cavity mode back into alignment. Reduced self-heating through more efficient operation and reduced thermal resistance should extend the bandwidth of oxide-confined VCSELs.

Large Signal Modulation

Large signal, digital modulation experiments were also performed using a 12Gb/s bit error rate tester and 26 GHz sampling oscilloscope. Figures 7 and 8 respectively show the dc light and voltage vs. current and frequency response for larger ~8x8 μm^2 multimode lasers which were initially investigated for large signal modulation. The link used the same photodetector as before with the addition of a ~9 dB, 18 GHz inverting amplifier. Eye diagrams and bit error rates were obtained

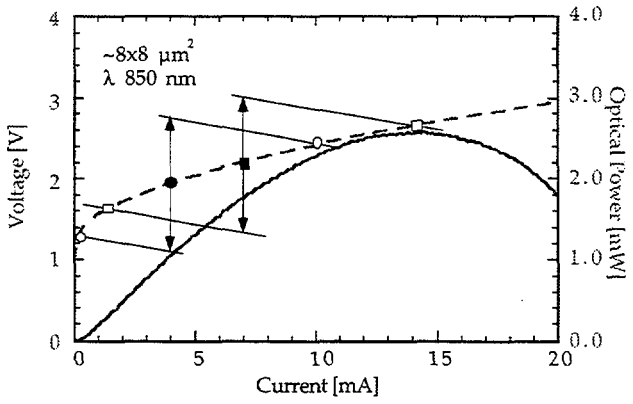

Figure 7. The light and voltage vs. Current characteristics for a multimode VCSEL. Bias and modulation conditions are indicated as discussed in the text.

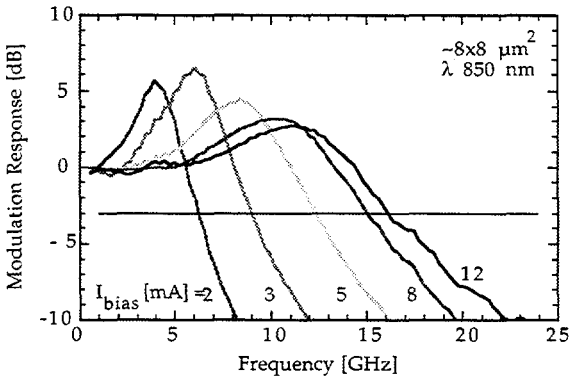

Figure 8. The modulation response of a multimode VCSEL for varying bias currents.

using a 2^7-1 pseudorandom bit sequence (PRBS). The short word length was necessitated by the 45 MHz low frequency cutoff of the amplifier. When the multimode laser was biased at 7 mA and modulated with emitter coupled logic (ECL) voltages as indicated by the squares in Figure 7, an open eye diagram was obtained up to 12 Gb/s as shown in Figure 9. Keeping in mind the signal level inversion caused by the amplifier, the pattern shows overshoot and ringing due to the multimode laser's relaxation resonance which is also apparent in the modulation response shown in Figure 8. Later experiments on the smaller single mode lasers showed much less overshoot due to the ability to drive those devices closer to a critically damped condition. The overshoot could of course be reduced by an appropriate electrical filter that limited the bandwidth further. Even without the filter, bit error rates as low as 10^{-13} were observed in preliminary investigations at 12 Gb/s.

Improved contrast ratios and simplified driving circuits motivate operating the laser so that the low drive level is below threshold if possible. Biasing the multimode laser at 4 mA, indicated by the circles in Figure 7, results in this mode of operation whereas the 7 mA bias was chosen to keep both levels above threshold. When biased at 4 mA, the turn-on delay associated with subthreshold operation resulted in significant pattern dependent jitter as seen in Figure 10 at 6 Gb/s. The extent of the jitter indicates an upper limit of about 1 Gb/s in these operating conditions.

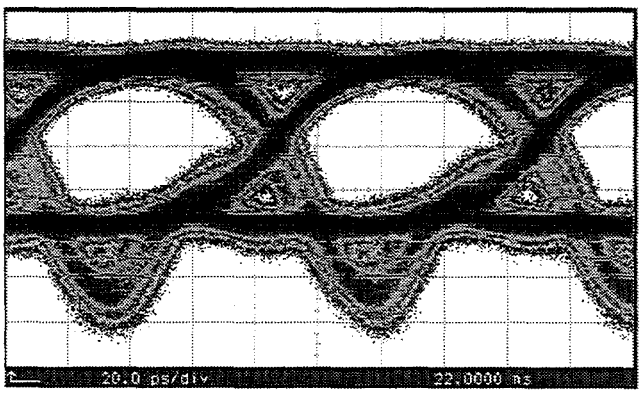

Figure 9. Eye diagram generated by 12Gb/s digital modulation of a multimode VCSEL biased at 7 mA linked to a photodetector and inverting amplifier without filtering.

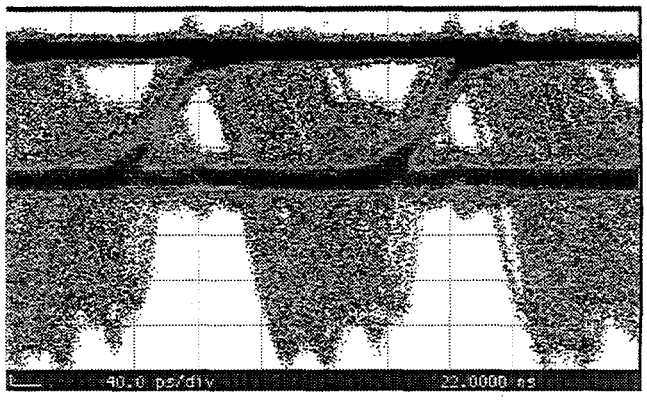

Figure 10. Eye diagram for the same configuration as in Figure 9 but biased at 4 mA and modulated at 6 Gb/s.

To further quantify the potential for these VCSELs to operate in this mode, the turn-on delay of both single mode and multimode lasers was measured for a variety of subthreshold biases. Pattern dependence was determined by using a repetitive pattern of 64 bits where only one bit was off. By varying the bit rate from 1 Gb/s to 12 Gb/s, the effect of off time on turn-on delay could be studied and used to infer the jitter associated with different lengths of off bit strings. The constant duty cycle approach reduces secondary effects due to varying heating or average bias level. Both the below threshold level and the high level were varied during the investigation.

Figure 11 shows the turn on delay as a function of the off time for the small single mode devices. Several curves are plotted for low levels of 0 V and 1 V and several different high levels ranging from 2.3 V (approximately 2 mA) to 3.8 V (approximately 4 mA). Note that these internal voltages are dropped across the 50 Ω source impedance in addition to the laser. The delay times for the two low levels are similar with the greatest difference occurring after short off times. When the high level is close to threshold, turn on maximum delay time can exceed 500 ps. Operation at several times threshold can make the delay as short as 120 ps. Still higher levels result in power saturation due to heating and give no shorter delay times.

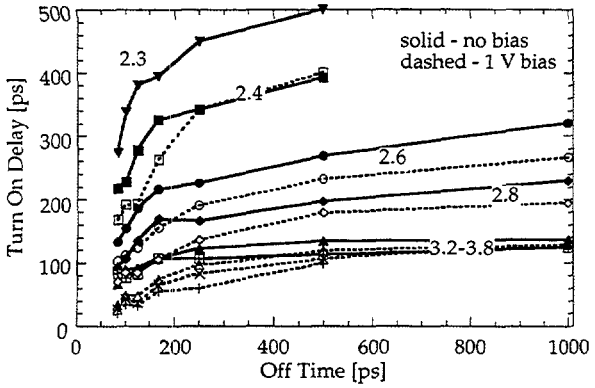

Figure 11. Turn on delay for a single mode VCSEL as a function of the preceding time off. The low (bias) and high levels are indicated for each curve.

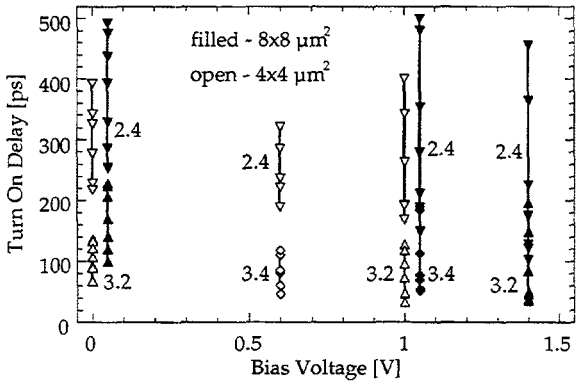

Figure 12. Ranges of turn on delay for varied off time and thus pattern dependent jitter are indicated for different bias and drive voltages.

The range of turn on delays for both the small and large lasers are summarized in Figure 11 to give an indication of pattern dependent jitter. The data is presented as a function of low level bias and grouped for a given high drive level. For long off times, the larger lasers are slightly slower at a given drive voltage. Increasing the low (bias) level doesn't substantially alter the turn on delay for long off times, but does shorten the delay after short off times. This is consistent with the subthreshold bias slowing carrier density decay from the active region but not providing enough steady state carrier concentrations to alter the turn on delay. The result is that subthreshold bias actually increases pattern dependent jitter but does not alter maximum turn on delay. Hence, 0 V bias is likely to be as attractive as higher levels of subthreshold bias.

Summary

While oxide confinement structures improve many parameters of VCSELs, it is also necessary to minimize the associated capacitance. Oxide confined VCSELs generate high photon densities by providing strong optical confinement and permitting operation to many times threshold through the combined benefits of low thresholds and high efficiency. The use of proton implantation has been described for reducing the oxide capacitance and increasing the electrical bandwidth beyond other factors. This has produced bandwidths up to 21.5 GHz at which point the present VCSELs are believed to be thermally limited. Additional improvements should be obtained with improved heatsinking and higher efficiencies. Structures can also be designed to minimize the detrimental effects of ion implantation on resistance and thus optimize the resistance vs. capacitance tradeoff.

Large signal modulation at data rates up to 12 Gb/s have been demonstrated. Despite these advances, below threshold bias still results in substantial turn on delay and pattern dependent jitter. To quantify the latter, turn on delay vs. off time under a variety of bias conditions has been studied and reported. Smaller, single mode devices do have lower turn-on times compared to large, multimode devices driven to the same number of times threshold.

Acknowledgments

The authors would like to thank C. Tigges for help in computer modeling of microwave circuits and F. Cajas and J. Nevers for technical assistance with measurements. This work was performed at Sandia, a multiprogram laboratory operated by Lockheed Martin for the United States Department of Energy. under Contract DE-AC04-94AL85000. K. Lear is presently with MicroOptical Devices Inc., 5601C Midway Park Pl. NE, Albuquerque, NM 87109 where this manuscript was prepared. M. Ochiai is presently with Hewlett Packard's Optoelectronics Division in San Jose, CA. J. Banas is presently with the

University of New Mexico, Center for High Technology Materials, Albuquerque, NM. J. Zolper is presently with the Office of Naval Research in Washington, DC. S. Kilcoyne is presently with Gore Photonics in Lompoc, CA.

References

[1] K. L. Lear, A. Mar, K. D. Choquette, S. P. Kilcoyne, R. P. Schneider, Jr., and K. M. Geib, "High-frequency modulation of oxide-confined vertical cavity surface emitting lasers", *Electron. Lett.* **32**(5), 457 (1996).

[2] K. D. Choquette, K. L. Lear, R. P. Schneider, Jr., K. M. Geib, J. J. Figiel, and R. Hull, "Fabrication and Performance of Selectively Oxidized Vertical-Cavity Lasers", *Photon. Tech. Lett.*, **7**(11), 1237 (1995).

[3] K. L. Lear, H. Q. Hou, J. J. Banas, B. E. Hammons, J. Furioli, and M. Osinski, "Vertical cavity laser on p-doped substrates", *Electron. Lett.* **33**(9), 783 (1997).

[4] B. J. Thibeault, K. Bertilsson, E. R. Hegblom, E. Strzelecka, P. D. Floyd, R. Naone, and L. A. Coldren, "High-Speed Characteristics of Low-Optical Loss Oxide-Apertured Vertical-Cavity Lasers", *Photon. Tech. Lett.*, **9**(1), 11 (1997).

Appendix C. Bibliography

This Appendix lists several recent publications related to this project. These publications were selected from the numerous publications/presentations produced during this project's duration. Together, they provide a good overview of the work performed on this project.

K. L. Lear, V. M. Hietala, H. Q. Hou, J. J. Banas, B. E. Hammons, J. C. Zolper, and S. P. Kilcoyne, "Small and large signal modulation of 850 nm oxide-confined vertical cavity surface emitting lasers," CLEO '97, Baltimore, MD, June 18, 1997.

V. M. Hietala, K. L. Lear, M. G. Armendariz, C. P. Tigges, H. Q. Hou, and J. C. Zolper, "Electrical Characterization and Application of Very High Speed Vertical Cavity Surface Emitting Lasers (VCSELs)," 1997 IEEE MTT-S International Microwave Symposium Digest, Denver, CO, Vol. 1, pp. 355-358, June 10, 1997.

K. L. Lear, H. Q. Hou, J. J. Banas, B. E. Hammons, J. Furioli, and M. Osinski, "Vertical-Cavity Lasers on p-Doped Substrates," Electronics Letters, 33(#9), pp. 783-784, 1997.

K. L. Lear, and R. P. Schneider, "Uniparabolic Mirror Grading for Vertical-Cavity Surface-Emitting Lasers," Applied Physics Letters, 68(#5), pp. 605-607, 1996.

K. L. Lear, A. Mar, K. D. Choquette, S. P. Kilcoyne, R. P. Schneider, and K. M. Geib, "High-Frequency Modulation of Oxide-Confined Vertical-Cavity Surface-Emitting Lasers," Electronics Letters, 32(#5), pp. 457-458, 1996.

K. L. Lear, R. P. Schneider, K. D. Choquette, and S. P. Kilcoyne, "Index Guiding Dependent Effects in Implant and Oxide Confined Vertical-Cavity Lasers," IEEE Photonics Technology Letters, 8(#6), pp. 740-742, 1996.

Distribution:

1	MS0188	LDRD Office, 4523
1	MS1079	A. D. Romig, 1300
1	MS0603	A. Owyoung, 1312
1	MS0603	T. E. Zipperian, 1313
1	MS0603	P. Esherick, 1314
1	MS0874	D. W. Palmer, 1342
10	MS0874	V. M. Hietala, 1342
5	MS0874	M. G. Armendariz, 1342
5	MS0603	K. D. Choquette, 1312

1	MS9018	Central Technical Files, 08940-2
2	MS0899	Technical Library, 04916
2	MS0619	Review & Approval Desk, 12690
		For DOE/OSTI